

Direct Detection of the Proton-Containing Group Coordinated to Mo(V) in the High pH Form of Chicken Liver Sulfite Oxidase by Refocused Primary ESEEM Spectroscopy: Structural and Mechanistic Implications

Andrei V. Astashkin,^{*,†} M. L. Mader, Andrew Pacheco, John H. Enemark,^{*} and Arnold M. Raitsimring^{*}

Contribution from the Department of Chemistry, University of Arizona, Tucson, Arizona 85721-0041

Received May 20, 1999. Revised Manuscript Received February 4, 2000

Abstract: A refocused primary electron spin–echo envelope modulation (RP ESEEM) technique and an adjustable frequency S/C-band pulsed EPR spectrometer have been used to produce ESEEM spectra with the lines due to nearby protons being greatly enhanced relative to those due to distant matrix protons. Application of this technique to the high pH (*hpH*) form of the Mo(V) center of sulfite oxidase has enabled nearby protons to be directly detected for the first time. Simulation of the RP ESEEM spectrum of the *hpH* form suggests the presence of two nearby protons that have distributed hyperfine interactions (hfi); these protons are ascribed to a Mo^V–OH group with strong H-bonding interactions to other nearby proton donors or to the presence of a coordinated H₂O ligand. The RP ESEEM technique promises to be widely applicable to the investigation of mutant forms of SO with altered Mo centers and paramagnetic centers in other metalloproteins where a nearby proton of interest is often masked by much more numerous distant protons and where high spectral resolution is not required. The distinctive differences in the CW and pulsed EPR spectra of the *lpH* and *hpH* forms are proposed to result from differences of the Mo^V–OH torsional angle and variations in the H-bonding interactions, which control the orientation of the Mo^V–OH proton(s) relative to the half-filled 4d_{xy} orbital. The large isotropic hfi for the *lpH* form is suggested to result from an intramolecular Mo^V–OH···S_{cys} hydrogen bonding interaction that places the proton of the Mo^V–OH group in the equatorial plane of the square pyramidal oxo-Mo(V) center of SO.

Introduction

Coupled electron–proton transfer¹ has long been postulated to be a key feature of the catalytic cycle of molybdoenzymes.² Thus, the ability to monitor protonation processes at the Mo centers of such enzymes is crucial for understanding their reaction mechanisms.^{3,4} Recently we investigated the coordination environment of the Mo(V) center of the high pH (*hpH*) form of sulfite oxidase (SO) in H₂O and D₂O solutions.⁵ In D₂O solution, the electron spin–echo envelope modulation (ESEEM) data definitively indicated the presence of a deuteron close to the Mo(V) center, which was ascribed to a Mo–OD group. However, all attempts to directly observe the corresponding nearby proton in H₂O solution were unsuccessful. These attempts included continuous wave X-band electron–nuclear double resonance (ENDOR) and two- and four-pulse ESEEM experiments at various operational frequencies (8–16 GHz). We hypothesized that the nearby proton was not directly observable because it does not occupy a unique position with respect to the Mo(V) center, and thus it gives rise to a statistical

distribution of proton hyperfine interaction (hfi) parameters. Such a distribution could well result in a substantial decrease in intensity of the proton lines in the ESEEM spectra. This situation is not unique; for example, the recent paper by Randall et al.⁶ shows that a nearby proton in a dinuclear Mn(III)Mn(IV) complex gives a barely detectable ESEEM signal that exhibits only about one tenth of the intensity expected from its hyperfine parameters. We also note that both pulsed and CW ENDOR techniques have provided examples of the detection of nearby strongly coupled protons and deuterons in paramagnetic transition metal centers.^{6–8} Possibly Davies ENDOR would have enabled detection of nearby protons for the *hpH* form of SO in H₂O. However, it is difficult to accurately quantitate the number of nuclei with ENDOR. Therefore we have focused our efforts on the development of ESE-based techniques for the detection and quantitation of nearby strongly coupled protons.

Here we describe advances in pulsed EPR methodology that have enabled us to detect the nearby protons in the *hpH* form of SO directly, and to determine the Mo···H interactions more accurately. This methodology also provides a means of minimizing the effects of instrumental dead time and substantially suppressing matrix proton lines. These two features should make

* Address correspondence to these authors.

† On leave from the Institute of Chemical Kinetics and Combustion, Russian Academy of Sciences, Novosibirsk 630090, Russia.

(1) Stiefel, E. I. *Proc. Natl. Acad. Sci. U.S.A.* **1973**, *70*, 988–992.

(2) Hille, R. *Chem. Rev.* **1996**, *96*, 2757–2816.

(3) Hille, R. ; JBIC, *J. Biol. Inorg. Chem.* **1997**, *2*, 804–809.

(4) Hille, R.; Rétey, J.; Bartlewski-Hof, U.; Reichenbecher, W.; Schink, B. *FEMS Micro. Rev.* **1999**, *22*, 489–501.

(5) Raitsimring, A. M.; Pacheco, A.; Enemark, J. H. *J. Am. Chem. Soc.* **1998**, *120*, 11263–11278.

(6) Randall, D. W.; Gelasco, A.; Caudle, M. T.; Pecororo, V. L.; Britt, R. D. *J. Am. Chem. Soc.* **1997**, *119*, 4481–4491.

(7) Tan, X.; Bernardo, M.; Thomann, H.; Scholes, C. P. *J. Chem. Phys.* **1993**, *98*, 5147–5157.

(8) Willems, J.-P.; Valentine, A. M.; Gurbiel, R.; Lippard, S. J.; Hoffman, B. M. *J. Am. Chem. Soc.* **1998**, *120*, 9410–9416.

this methodology widely applicable to pulsed EPR analysis of biological samples in general.

Minimizing the intrinsic dead time in pulsed-EPR spectrometers poses a well-known and complicated technical problem for which no universal solution is available.^{9–13} The direct suppression of proton matrix lines has never been considered in ESEEM theory, although in some cases, an indirect approach that utilizes blind spots in multi-pulse sequences has been used for this purpose.^{14,15} It was shown by Grupp et al.¹⁶ that a simple three-pulse sequence implementing a refocusing of the primary echo signal allows drastic reduction of the dead time in primary ESEEM measurements. Recently we have shown that this pulse sequence, in combination with judicious adjustment of the operational frequency, leads to significant suppression of the matrix proton line relative to the line of nearby protons.¹⁷ Conceptually similar techniques were previously used in pulsed ENDOR measurements.^{18,19} The complete theory and experimental realization of the refocused primary (RP) echo are described elsewhere.¹⁷ Here we present only the theoretical background necessary for understanding the RP ESEEM results obtained for the *hpH* form of SO. The implications of these new results for the structures of the *hpH* and *lpH* forms of SO and the mechanism of SO are also discussed.

Experimental Section

Samples of highly purified SO were prepared in the *hpH* (in H₂O and D₂O buffers) and phosphate inhibited (*Pi*) forms as previously described.^{5,20} The experiments were performed on the S/C band pulsed EPR spectrometer described elsewhere²¹ at a temperature of about 20 K. The duration of all microwave (m.w.) pulses was 20 ns, and the two-dimensional (2D) data consisted of 80 × 80 points collected with 20 ns steps along both time coordinates (τ and T , see below). To suppress unwanted spin-echo signals, four step phase cycling (0°–90°–180°–270°) for the second pulse was employed. The duration of one 2D experiment was about 3 h.

Results and Discussion

RP ESEEM Spectra. The pulse sequence for refocusing of the primary ESE signal consists of three m.w. pulses (Figure 1). The first two pulses are separated by the time interval τ and form a primary ESE (PE) signal at the time 2τ . The third pulse, with a nominal flip angle of 180°, is applied at a time T after

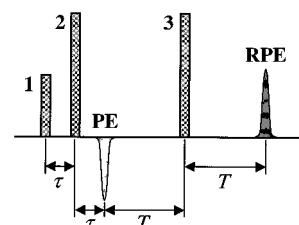


Figure 1. The pulse sequence for detecting the RP ESE. “1”, “2”, and “3” denote the m.w. pulses. “PE” and “RPE” denote the conventional primary and RP ESE signals, respectively.

2τ to refocus the primary echo (RPE) signal at the time $2(\tau + T)$. Although this technique still suffers from the dead time problem along the T coordinate, virtually zero dead time is achieved along the τ coordinate. An experiment in which both τ and T are varied results in a two-dimensional (2D) RP ESEEM, $V(\tau, T)$. A Fourier transform (FT) of $V(\tau, T)$ gives a 2D spectrum $V(\nu, \nu')$, in which the time intervals τ and T translate into the frequencies ν and ν' , respectively. The 2D spectrum shows some useful correlations between various ESEEM harmonics, but a discussion of these correlations is beyond the scope of this paper and details have been reported elsewhere.¹⁷ Here we utilize only one feature relevant to the problem. It was found that integration of $V(\tau, T)$ over T gives

$$V(\tau) = 1 - \frac{k}{4} \left[3 - \cos(2\pi\nu_\alpha) - \cos(2\pi\nu_\beta) + \frac{1 + \sqrt{1-k}}{2} \cos(2\pi\nu_\delta) + \frac{1 - \sqrt{1-k}}{2} \cos(2\pi\nu_\sigma) \right] \quad (1)$$

where ν_α and ν_β are the nuclear transition frequencies at the α and β electron spin manifolds, $\nu_\sigma = \nu_\alpha + \nu_\beta$ and $\nu_\delta = \nu_\alpha - \nu_\beta$ are the sum and difference combination frequencies, respectively, and k is the usual factor describing the ESEEM amplitude.²²

As seen from eq 1, the amplitude of the ν_σ harmonic depends nonlinearly on the factor k . When $0 < k \ll 1$, the ν_σ amplitude is proportional to k^2 , and when $k \sim 1$ it is proportional to k . In turn, $k \propto T_\perp^2$. For distant protons $k \ll 1$, and the amplitude of their ν_σ harmonic in the integrated RP ESEEM (eq 1) will be much less than in the ESEEMs obtained with two- or four-pulse techniques. On the other hand, for a nearby proton, $k \sim 1$ can be achieved under conditions in which mutual cancellation of the Zeeman and hyperfine interactions occurs at one of the electron spin manifolds. In the case of anisotropic hfi, this corresponds to the situation in which the nuclear Zeeman frequency is somewhere between T_\perp and $2T_\perp$.

For the particular case of the *hpH* form of SO, based on the data for T_\perp obtained from a deuterated sample,⁵ the cancellation condition should be achieved at operational frequencies ν_0 between ~ 3.2 and 6 GHz. At the same time, even at the lowest ν_0 of 3.2 GHz, k for the distant matrix protons would not exceed 5×10^{-2} , so that the modulation from distant protons should be substantially suppressed.

In accord with these considerations, after several preliminary experiments in the 3–6 GHz range of operational frequencies, we found that optimal conditions correspond to ν_0 of 5.3–5.5 GHz. The field-sweep ESE spectrum of the *hpH* form of SO in H₂O detected at $\nu_0 = 5.404$ GHz is shown in Figure 2a, and the cosine FT spectrum of the integrated RP ESEEM is shown in Figure 2b (trace 3). This spectrum shows an intense narrow peak at the frequency of 8.38 MHz coinciding with the Zeeman

- (9) Davis, J. L.; Mims, W. B. *Rev. Sci. Instrum.* **1981**, *52*, 131.
 (10) Narayana, P. A.; Massoth, R. J.; Kevan, L. *Rev. Sci. Instrum.* **1983**, *53*, 624.
 (11) Mims, W. *J. Magn. Reson.* **1984**, *59*, 291.
 (12) Schweiger, A.; Ernst, R. R. *J. Magn. Reson.* **1988**, *77*, 512.
 (13) Borbat, P. P.; Crepeau, R. H.; Freed, J. H. *J. Magn. Reson.* **1997**, *127*, 155.
 (14) Dikanov, S. A.; Astashkin, A. V.; Tsvetkov, Y. D. *Chem. Phys. Lett.* **1988**, *144*, 251.
 (15) Astashkin, A. V.; Dikanov, S. A.; Tsvetkov, Y. D. *Chem. Phys. Lett.* **1988**, *144*, 258.
 (16) Grupp, A.; Shanmin, A.; Mehring, M. Deadtime Free Echo Modulation in Pulsed EPR. In *Congress Ampere on Magnetic Resonance and Related Phenomena, Extended Abstracts*; Proceedings of Congress Ampere on Magnetic Resonance and Related Phenomena, Stuttgart, 1990; Mehring, M., von Schütz, J. U., Wolf, H. C., Eds.; Springer-Verlag: Berlin: Stuttgart, 1990; p 454.
 (17) Astashkin, A. V.; Raitsimring, A. M. *J. Magn. Reson.* **2000**, *142*, 280–291. Astashkin, A. V.; Enemark, J. H.; Pacheco, A.; Raitsimring, A. M. *Abstracts of 41st Rocky Mountain Conference on Analytical Chemistry*; Denver, CO, August 1–5, 1999; Abstract 51, p 47.
 (18) Astashkin, A. V.; Kawamori, A.; Koderia, Y.; Kuroiwa, S.; Akabori, K. *J. Chem. Phys.* **1995**, *102*, 5583.
 (19) Doan, P. E.; Hoffman, B. M. *Chem. Phys. Lett.* **1997**, *269*, 208.
 (20) Pacheco, A.; Basu, P.; Borbat, P.; Raitsimring, A. M.; Enemark, J. H. *Inorg. Chem.* **1996**, *35*, 7001–7008.
 (21) Astashkin, A. V.; Kozlyuk, V.; Raitsimring, A. M. *Abstracts of 40th Rocky Mountain Conference on Analytical Chemistry*; Denver, CO, July 26–30, 1998. Additional materials.

(22) Dikanov, S. A.; Tsvetkov, Y. D. *Electron Spin-Echo Modulation (ESEEM) Spectroscopy*; CRC Press: Boca Raton, FL, 1992.

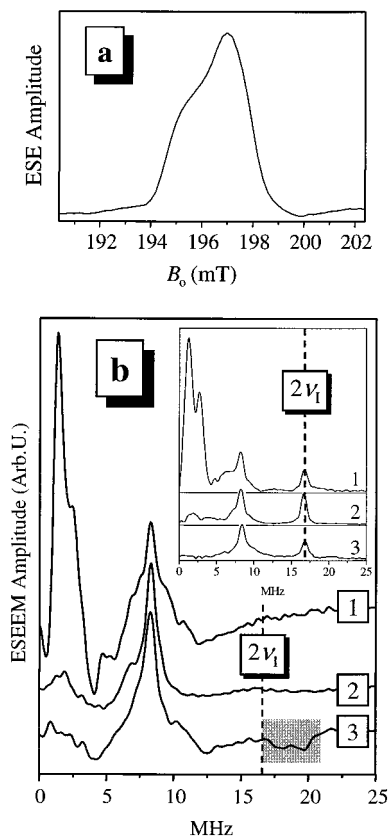


Figure 2. (a) Field-sweep ESE spectrum of the *hpH* form in H₂O detected at $\nu_0 = 5.404$ GHz. (b, main panel) Cosine FT spectra of the experimental integrated RP ESEEM of different forms of SO: trace 1, *hpH* form in D₂O; trace 2, *Pi* form in H₂O; trace 3, *hpH* form in H₂O. The shaded area marks the region of the proton sum combination line. Experimental conditions: trace 1, $\nu_0 = 5.383$ GHz, $B_0 = 195$ mT; trace 2, $\nu_0 = 5.387$ GHz, $B_0 = 194.4$ mT; trace 3, $\nu_0 = 5.404$ GHz; $B_0 = 197$ mT. Measurement temperature, 18 K. Inset: Magnitude FT spectra for the primary ESEEM for *hpH* form in D₂O (trace 1), *Pi* form of SO in H₂O (trace 2), and *hpH* form in H₂O (trace 3).

frequency of protons in the applied magnetic field $B_0 = 197$ mT. This peak is characteristic of distant protons abundant in the protein backbone. The broad shoulders around this peak are, at least partly, contributed by the transition lines of nearby protons that are the subject of primary interest of this work. In addition, the spectrum distinctly shows a broad sum combination line (easily recognizable by the negative sign of its amplitude, see eq 1) in the frequency range from 17 to 20.5 MHz, with slight intensity enhancements at 17.8 and 19.7 MHz (shaded area of trace 3).

To verify the assignment of the broad features in the shaded area of trace 3 (Figure 2b) to nearby protons, we performed additional experiments on two other systems that do *not* have a proton-containing group coordinated to Mo(V): the *hpH* form of SO in buffered D₂O solution and the phosphate inhibited (*Pi*) form.^{5,20} The cosine FT spectra of the RP ESEEM for these two forms of SO are also presented in Figure 2b. Neither the *hpH* form in D₂O (trace 1) nor the *Pi* form (trace 2) exhibit the broad negative ν_σ line at 17 to 20.5 MHz observed for the *hpH* form in H₂O (trace 3), further substantiating the assignment of this line to nearby protons.

The spectra of *hpH*/D₂O and *Pi* forms of SO *do* show some broad features around the matrix proton Zeeman peak. The origin of these features, however, is different in all three spectra. In the *hpH*/D₂O form these broad features represent sum and difference combinations of the proton Zeeman line with the

extremely intense lines of deuterons from the D₂O buffer situated in the low-frequency range (below 4.6 MHz, see trace 1 in Figure 2b). In the *Pi* form the low-frequency shoulder of the proton Zeeman line might be partly contributed by the ³¹P transition at the cancellation condition.²⁰ In addition, the methylene protons of the cysteine residue coordinated to the Mo(V) center in all three samples of SO²³ may also make some contribution to the broad feature around the proton Zeeman line.

The effectiveness of RP ESEEM for suppressing the intense ν_σ line due to distant protons is illustrated by comparison of the RP ESEEM spectra in the main panel of Figure 2b with their corresponding primary ESEEM spectra shown in the inset of Figure 2b. For all three forms of SO the RP ESEEM method completely suppresses the intense ν_σ line due to distant protons. The primary ESEEM spectrum of the *hpH* form (trace 3 in the inset) shows some evidence for the broad ν_σ line near 20 MHz, due to nearby protons, but it is much less pronounced because of the dead time of about 200 ns and because the intense ν_σ line due to distant matrix protons obscures its observation.

The results summarized in Figure 2b indicate that the broad sum combination line observed in the RP ESEEM spectra of the *hpH* form of SO in H₂O can only be attributed to exchangeable protons close to Mo(V). To obtain quantitative information about the number of nearby protons and their hfi parameters, we have performed numerical simulations of the integrated RP ESEEM spectra in the same manner as was described previously.^{5,20} The only difference is that the basic expressions that describe the primary and four-pulse ESEEM have been substituted in a code for eq 1, describing the primary refocused ESEEM. In the simulations we used the experimental *g*-values of the EPR spectrum of Mo(V) in *hpH* ($g_x = 1.953$, $g_y = 1.964$, and $g_z = 1.988$).²⁴ The geometrical parameters for the Mo–OH fragment (Mo–O = 2.1 Å, O–H = 0.96 Å; Mo–O–H = 110°)²⁵ give a Mo···H distance of about 2.6 Å. This distance, however, was not used in the calculations directly to determine the dipolar interaction of the OH proton because this interaction is considerably influenced by spin polarization of the Mo–O and O–H bonds and the oxygen atomic orbitals. The proton anisotropic hyperfine coupling constant T_\perp , therefore, was a variable parameter in the simulation. The geometry of the Mo–O–H fragment was, however, used for calculation of the secular and nonsecular parts of the anisotropic hfi for various orientations of magnetic fields \mathbf{B}_0 . The set of these orientations was determined by our observation position in the EPR spectrum (close to g_y) with the *g*-tensor given above.

The initial approximation for the simulations was based upon the parameters estimated previously from the study of *hpH* SO in D₂O buffer.⁵ That is, the orientation of the Mo···H radius-vector in the *g*-frame was determined by the direction cosines (0.583, 0.694, 0.423). The anisotropic hfi was considered to be uniformly distributed within the limits from -7.5 to -8.5 MHz, as obtained from the corresponding limits for a deuteron (-1.15 to -1.3 MHz).⁵ The result of the RP ESEEM simulation with these parameters is shown by trace 2 in Figure 3. One can see that the sum combination line (shaded area) in trace 2 is situated at noticeably higher frequencies than in the experimental spectrum (trace 1). This implies that the anisotropic hfi was somewhat overestimated in the previous work,⁵ which is not

(23) Kisker, C.; Schindelin, H.; Pacheco, A.; Webbi, W. A.; Garrett, R. M.; Rajagopalan, K. V.; Enemark, J. H.; Rees, D. C. *Cell* **1997**, *91*, 973–983.

(24) Lamy, M. T.; Gutteridge S.; Bray, R. C. *Biochem. J.* **1980**, *185*, 397–403.

(25) Bohmer, J.; Haselhorst, G.; Wieghardt, C.; Nuber, B. *Angew. Chem. Int. Ed. Engl.* **1994**, *33*, 1473–1476.

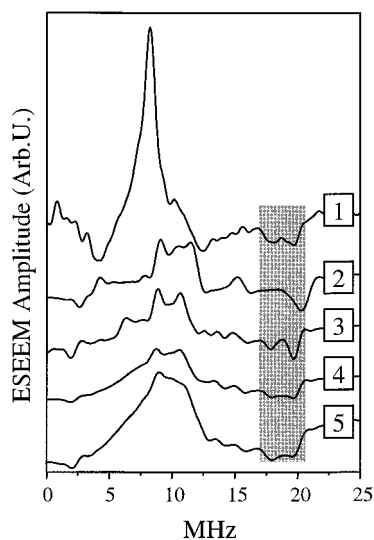


Figure 3. Cosine FT spectra of the integrated RP ESEEM. Trace 1: Experimental spectrum of the *hpH* form in H₂O. Trace 2: Simulated spectrum for a single close proton, with the Mo \cdots H orientation in the *g*-frame determined by the direction cosines (0.583, 0.694, 0.423) and the anisotropic hfi uniformly distributed within the limits from -7.5 to -8.5 MHz. Trace 3: Similar simulation for a single close proton with two equiprobable values of the anisotropic hfi constants, -4 and -7.6 MHz. Trace 4: Simulation for a single proton in the uniform rotational distribution model (see text for details of the Mo–O–H fragment geometry and eq 2 for related T_{\perp} distribution). Trace 5: Similar simulation for two protons. The absence of the narrow intense line at the proton Zeeman frequency (~ 8.3 MHz) in the simulated traces is due to the fact that distant protons were not included in the simulations.

surprising because of complications associated with the nuclear quadrupole interaction of deuterons combined with their low magnetic moment.

The sum combination line in the experimental spectrum (trace 1 in Figure 3) appears to be contributed by two poorly resolved peaks with maxima at 17.9 and 19.7 MHz. Therefore, the next attempt to simulate this spectrum assumed two types of statistically distributed Mo(V) sites. Each site had one nearby proton, but the relative positions of the protons in the two sites were allowed to be slightly different, thereby giving rise to two different anisotropic hfi constants of -4 MHz and -7.6 MHz. Trace 3 of Figure 3 shows that the simulated spectrum, obtained with the assumption that these two T_{\perp} values have equal probabilities, reproduces the correct positions for the sum combination line. However, the resolution of these peaks in the simulated spectrum is considerably higher than in the experimental one.

To decrease the resolution between the peaks constituting the sum combination line, some kind of a distribution of the anisotropic hfi must be introduced within the above limits, and with enhancement of the statistical weights at the ends of the range. It is also clear that this distribution should be associated with some local structural disorder in the system. Fortunately, there is a simple physical model, which provides the required local structural disorder and directly associates it with the distribution of the anisotropic hfi. In this model, the position of the Mo–O bond is fixed in the molecular and *g*-frames. The positions of the –OH protons are uniformly distributed over the circle obtained by rotation of the –OH fragment around the Mo–O bond. The dihedral angle (γ) is defined as the angle between the plane of the Mo(V) d_{xy} orbital and the Mo–O–H plane. The distribution of this dihedral angle represents the local structural disorder mentioned above. To reproduce the specific

shape of the ν_{σ} line in the RP ESEEM spectrum of *hpH* SO (trace 3 in Figure 2), we have to introduce a dependence of the anisotropic hfi constant T_{\perp} on γ :

$$T_{\perp} = -5.7 - 1.6 \cos(2\gamma) = -4.1 - 3.2 \cos^2(\gamma) \text{ [MHz]} \quad (2)$$

This kind of dependence of anisotropic hfi on γ was previously found for a hydroxyl proton in a C–OH radical fragment.²⁶ Here we assume that a qualitatively similar dependence might be expected for the Mo–OH fragment since the electron spin distribution has approximate C_{2v} symmetry with respect to the C–O bond in the C–OH radical fragment and with respect to the Mo–O bond in the Mo–OH fragment. The outlined model will be briefly referred to as the uniform rotational distribution model.

A typical simulation result is shown by trace 4 in Figure 3. The simulated spectrum reproduces the broad fundamental line with positive amplitude and the sum combination line with negative amplitude, which has a characteristic two-peak shape. The peak positions correspond to $\gamma = 0^{\circ}$ (180°) and 90° (270°). This particular simulation has been performed for $\theta = 45^{\circ}$ and $\varphi = 0^{\circ}$. Similar spectra were also obtained for other values of θ and φ (not shown). Therefore, our simulations at g_y were not sensitive to the Mo–O bond orientation in the *g*-frame.

The amplitude of the lines from the nearby proton in the calculated trace 4 in Figure 3 is somewhat smaller than the experimental amplitude. This result stimulated us to investigate the possibility of two nearby protons being associated with the equatorial O atom (trace 5, Figure 3). The corresponding simulation model for two protons is similar to that discussed above. It assumed a planar Mo–OH₂ unit with the second proton being situated at the dihedral angle $\gamma + 180^{\circ}$. The general appearance of the RP ESEEM spectrum of trace 5 is similar to those of traces 1 and 4, but the amplitudes of the simulated spectrum features of trace 5 are closer to those found in the experimental trace 1.

The indication from the simulations of the RP ESEEM that the *hpH* Mo(V) center may be associated with two nearby protons (trace 5, Figure 3) instead of one (as was assumed previously⁵) made it essential to investigate how this two-proton model would fit the experimental data obtained earlier for the *hpH* form of SO in D₂O buffer. Trace 1 in Figure 4 corresponds to Figure S3(f) in ref 5 and shows the amplitude FT spectrum of the primary ESEEM of the *hpH* form of SO in D₂O buffer. To obtain this spectrum, the primary ESEEM recorded in the previous work⁵ at $\nu_{\sigma} = 15.237$ GHz, $B_0 = 554.3$ mT (i.e., at $g = g_y$), the same position as in the present RP ESEEM measurements) was Fourier transformed after the elimination of the contribution of distant matrix deuterons (for details, see ref 5). The broad line centered at about 3.6 MHz in this spectrum is contributed by the fundamental lines of nearby deuteron(s), and the narrow line at about 7.4 MHz is the sum combination peak. Trace 2 in the same figure represents the result of the simulation for a single nearby deuteron with the hfi/nqi parameters estimated in the previous work.⁵ The intensities of the prominent features in both spectra show good overall agreement.

Trace 3 in Figure 4 shows the result of the simulation for two nearby deuterons using the uniform rotational distribution model with T_{\perp} recalculated for deuterons from eq 2 and the same nuclear quadrupole coupling constant, as in ref 5 (the electric field gradient was assumed to be parallel to the OD

(26) Schastnev, P. V.; Lihoshertov, V. M.; Musin, R. N. *Zh. Strukt. Khim.* **1974**, *15*, 554–560.

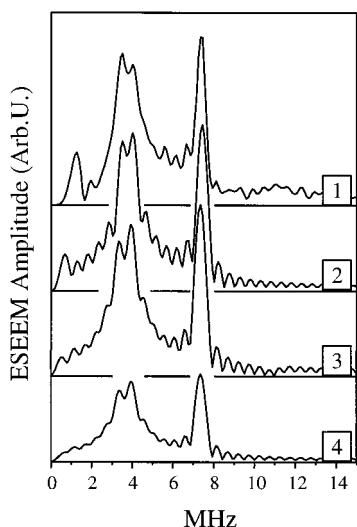


Figure 4. Amplitude FT spectra of the primary ESEEM of the *hpH* form of SO in D₂O buffer. Trace 1: Experimental spectrum at $\nu_0 = 15.237$ GHz, $B_0 = 554.3$ mT. Trace 2: Simulated spectrum for a single close deuteron with hfi/nqi parameters, taken from ref 5. Trace 3: Simulated spectrum for two deuterons in the uniform rotational distribution model with $T_{\perp} = -0.876 - 0.246 \cos(2\gamma)$ [MHz] as recalculated from eq 2 for a deuteron (corresponds to the RP ESEEM simulation for two protons shown by trace 5 in Figure 3). The quadrupole coupling constants in this simulation were the same as in ref 5 (with the electric field gradients aligned with the OD bonds). Trace 4: Similar simulation for single deuteron (corresponds to trace 4 in Figure 3).

bond). This spectrum is also in good agreement with the experimental one. However, the spectrum simulated for a single close deuteron (OD) using the uniform rotational distribution model (trace 4 in Figure 4) gives spectral line intensities that are substantially lower than those in the experimental spectrum. Thus, the structural model that includes two protons located in close proximity to the Mo(V) center, with the distribution of hfi parameters described above, fits well with the experimental data obtained previously for the *hpH* form in D₂O.⁵

Figure 4 also illustrates that both the intensity of the sum combination line and the magnitude of the anisotropic hfi must be considered in determining the number of nearby nuclei from ESEEM measurements. For deuterons the shifts of the sum combination line are small and are mixed with the shifts/splittings caused by the quadrupole interaction. For the *hpH* form of SO the deuteron data by themselves cannot distinguish between the single nearby deuteron model of trace 2 and the rotationally distributed two deuteron model of trace 3. Protons have no quadrupole interaction and have sum combination line shifts that are 6.5 times larger than those for deuterons. This paper clearly shows that low-frequency ESEEM investigation of a protonated sample using the new pulse technique with nonlinear response of the intensities to the anisotropic hfi is more sensitive to the number of nearby nuclei than previous techniques employing deuterated samples.

In this analysis of nearby protons in the *hpH* form of SO, it is also important to recall the fact that no sum combination features due to nearby protons were observed in the primary ESEEM spectra detected at X-band.⁵ To check whether this new two-proton model is in agreement with the X-band experimental data, we also performed simulations of the X-band primary ESEEM proton spectra. It was found that the intensity of the sum combination line falls below the noise level (0.5–0.7% in those experiments), if an additional narrow (0.5 MHz) Gaussian distribution of T_{\perp} is added to that produced by the uniform

rotational model. This additional, purely statistical, distribution smooths the spectrum singularities accentuated by the rather large dead time used in the primary ESEEM experiment. Introduction of such a narrow distribution does not affect the RP ESEEM spectra discussed above. Therefore, this slightly updated model satisfactorily describes all previous experimental data.

The uniform rotational distribution of the proton position was used in the above spectral simulations as a convenient model to automatically provide the distribution of T_{\perp} with the required properties of (i) enhancements of the statistical weight for $T_{\perp} \approx -4.1$ and -7.3 MHz and (ii) nonzero, though smaller, statistical weights for T_{\perp} between these two limiting values. We may note, however, that any structural disorder of the Mo^V–OH_{*n*} (*n* = 1,2) fragment producing the distribution of T_{\perp} with the described properties will result in similar ESEEM spectra and similar conclusions as to the number of nearby protons.

Implications for the Mechanism of Sulfite Oxidase. The RP ESEEM results discussed above for the *hpH* form of SO provide the first direct detection and quantitation of nearby protons for this form of the enzyme. The implications of these new RP ESEEM results for the reaction mechanism of SO will next be considered. The crystal structure of sulfite oxidase²³ shows that the molybdenum center has approximate square-pyramidal geometry (1 of Figure 5) and is buried at the bottom of a positively charged pocket that provides an “electrostatic bulls-eye”²⁷ relative to the surrounding protein surface, which is predominantly neutral or negatively charged. This positively charged bulls-eye favors binding of the anionic substrate, sulfite. The equatorial oxygen atom of the Mo center is exposed to the solvent near the center of the bulls-eye and is proposed to be transferred to sulfite to form sulfate during turnover.^{28–30} The Mo center is reoxidized by sequential intramolecular electron transfer (IET) to the *b*-type heme center of SO; in the crystal structure of SO the Mo•••Fe distance is ~ 32 Å.

Figure 5 shows a detailed mechanism for the chemical changes that are thought to occur at the Mo center of SO during turnover. Figure 5 incorporates specific features of several previously proposed mechanisms,^{28–30} information from the X-ray crystal structure,²³ Mo K-edge EXAFS,^{31–34} CW-EPR,^{24,34–40} resonance Raman,⁴¹ ESEEM studies of other forms of SO,^{5,20} steady-state and stopped-flow kinetics,²⁹ flash photolysis studies of the rates of intramolecular electron trans-

(27) Hazzard, J. T. Private communication.

(28) Rajagopalan, K. V. *Molybdenum and Molybdenum Containing Enzymes*; Coughlan, M., Ed.; Pergamon: Oxford, 1980; pp 241–272.

(29) Brody, M. S.; Hille, R. *Biochemistry* **1999**, *38*, 6668–6677.

(30) Pacheco, A.; Hazzard, J. T.; Tollin, G.; Enemark, J. H. *JBIC, J. Biol. Inorg. Chem.* **1999**, *4*, 390–401.

(31) George, G. N.; Pickering, I. J.; Kisker, C. *Inorg. Chem.* **1999**, *38*, 2539–2540.

(32) George, G. N.; Kipke, C. A.; Prince, R. C.; Sunde, R. A.; Enemark, J. H.; Cramer, S. P. *Biochemistry* **1989**, *28*, 5075–5080.

(33) George, G. N.; Garrett, R. M.; Prince, R. C.; Rajagopalan, K. V. *J. Am. Chem. Soc.* **1996**, *118*, 8588–8592.

(34) George, G. N.; Garrett, R. M.; Graf, T.; Prince, R. C.; Rajagopalan, K. V. *J. Am. Chem. Soc.* **1998**, *120*, 4522–4523.

(35) Kessler, D. L.; Rajagopalan, K. V. *J. Biol. Chem.* **1972**, *247*, 6566.

(36) Kessler, D. L.; Rajagopalan, K. V. *Biochim. Biophys. Acta* **1974**, *370*, 389.

(37) Bray, R. C.; Lamy, T.; Gutteridge, S.; Wilkinson, T. *Biochem. J.* **1982**, *201*, 241–243.

(38) George, G. N. *J. Magn. Reson.* **1985**, *64*, 384–394.

(39) Cleland, W. E., Jr.; Barnhart, K. M.; Yamanouchi, K.; Collison, D.; Mabbs, F. E.; Ortega, R. B.; Enemark, J. H. *Inorg. Chem.* **1987**, *26*, 1017–1025.

(40) George, G. N.; Prince, R. C.; Kipke, C. A.; Sunde, R. A.; Enemark, J. H. *Biochem. J.* **1988**, *256*, 307.

(41) Garton, S. D.; Garrett, R. M.; Rajagopalan, K. V.; Johnson, M. K. *J. Am. Chem. Soc.* **1997**, *119*, 2590–2591.

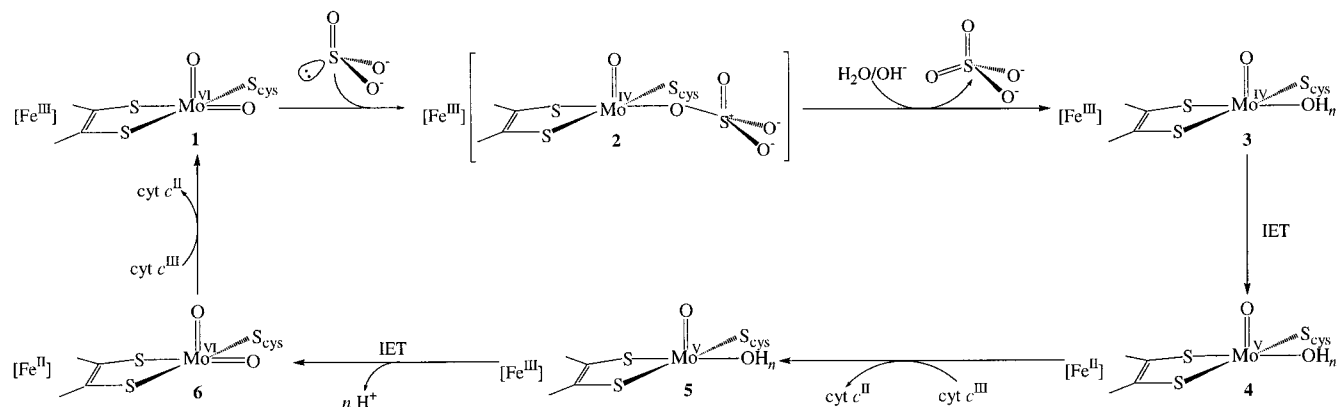


Figure 5. Composite mechanism proposed for sulfite oxidase. The coordination about the Mo center is based upon the X-ray structure and EXAFS results for the fully oxidized enzyme (**1**); the oxidation state of the Fe atom of the *b*-type heme center for each step in the proposed sequence is shown to the left of each structure. Nucleophilic attack on the equatorial Mo^{VI}=O group by sulfite is postulated to generate a Mo^{IV}-OSO₃ species²⁹ (**2**) that reacts with OH⁻ or H₂O to release sulfate (product) and generate **3**. Intramolecular electron transfer (IET) gives the Fe^{II}/Mo^V-OH_{*n*} (*n* = 1 or 2) species (**4**) that have been investigated by EPR and which are the subject of this work. During turnover sequential one-electron oxidations of **4** by oxidized cytochrome *c*, passing through **5** and **6**, regenerate the fully oxidized resting enzyme (**1**).

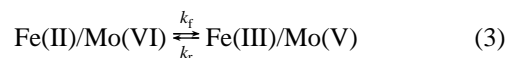
Table 1. EPR Data for Sulfite Oxidase

	g values				A(¹ H), 10 ⁻⁴ cm ⁻¹				ref.
	1	2	3	av.	1	2	3	av.	
SO (low pH form)	2.007	1.974	1.968	1.983	8.0	7.4	11.9	9.1	24, 48, 49
SO (high pH form)	1.990	1.966	1.954	1.970					24, 48, 49
SO (phosphate inhibited form)	1.992	1.969	1.961	1.978					24

fer,^{30,42,43} and theoretical studies of oxo-transfer reactions.^{44,45} Structure **1** of Figure 5 depicts the Mo coordination of the fully oxidized resting enzyme as determined from the X-ray structure of SO²³ and XAS and EXAFS studies of polycrystalline oxidized SO;³¹ Fe^{III} represents the distant *b*-type cytochrome center of SO. Nucleophilic attack on the equatorial Mo^{VI}=O group of the Mo^{VI}O₂ center of **1** by the lone pair on the S atom of sulfite²⁹ leads to an oxo-Mo^{IV}-OSO₃ complex (**2**) that reacts rapidly with water or hydroxide to give an oxo-Mo^{IV}-OH_{*n*} (*n* = 1, 2) center (**3**). IET to the *b*₅-type heme generates an oxo-Mo^V-OH_{*n*} center (**4**) that gives rise to the well-known Mo(V) EPR signals that are dependent upon pH and anions (Table 1).^{24,46-47} Reaction with two molecules of oxidized cytochrome *c* and loss of the proton(s) from Mo^V-OH_{*n*} complete the catalytic cycle and regenerate the starting dioxo-Mo(VI) center (**1**). A recent comprehensive study of the kinetic behavior of chicken liver SO supports the mechanism of Figure 5;²⁹ *k*_{red} (nucleophilic attack by the substrate on the Mo^{VI}O₂ unit) is principally rate limiting above pH 7 and is independent of pH, at least in the absence of small anions. The mechanism of Figure 5 is also supported by experimental⁵⁰⁻⁵⁹ and theoretical^{44,45} studies of

the reactions of phosphines with complexes possessing *cis*-Mo^{VI}O₂ centers.

Recently we reported a detailed study of the kinetics of IET between the Mo and heme centers of SO that showed the rates of both the forward and reverse reactions of eq 3 to be strongly



dependent upon pH and the concentration of small anions.³⁰ Structures **5** and **6** of Figure 5 were the starting point for a mechanistic analysis of these results that also considered how the equatorial Mo^V-OH group of **5** would be affected by the immediate surroundings of the active site, especially the positively charged anion binding pocket of SO (Schemes 2 and 3 of ref 30). It was proposed that equilibria involving the relative concentrations of hydroxide and small anion (X^{*n*-}) in the positively charged binding pocket could affect the observed rate for IET. In particular, low pH buffers containing high concentrations of small anions should favor an enzyme form in which an anion occupies the pocket (**7**), whereas high pH buffers with low concentrations of small anions should favor a form in which OH⁻ occupies the pocket (**8**). Faster IET is observed in high pH buffers containing low concentrations of small anions

(42) Kipke, C. A.; Cusanovich, M. A.; Tollin, G.; Sunde, R. A.; Enemark, J. H. *Biochemistry* **1988**, *27*, 2918-2926.

(43) Sullivan, E. P., Jr.; Hazzard, J. T.; Tollin, G.; Enemark, J. H. *Biochemistry* **1993**, *32*, 12465-12470.

(44) Pietsch, M. A.; Hall, M. B. *Inorg. Chem.* **1996**, *35*, 1273-1278.

(45) Izumi, Y.; Rose, K.; Glaser, T.; McMaster, J.; Basu, B.; Enemark, J. H.; Hedman, B.; Hodgson, K. O.; Solomon, E. I. *J. Am. Chem. Soc.* **1999**, *121*, 10035-10046.

(46) Gutteridge, S.; Lamy, M. T.; Bray, R. C. *Biochem. J.* **1980**, *191*, 285-288.

(47) Bray, R. C.; Gutteridge, S.; Lamy, M. T.; Wilkinson, T. *Biochem. J.* **1983**, *211*, 227-236.

(48) Dhawan, I. K.; Pacheco, A.; Enemark, J. H. *J. Am. Chem. Soc.* **1994**, *116*, 7911-7912.

(49) Dhawan, I. K.; Enemark, J. H. *Inorg. Chem.* **1996**, *35*, 4873-4882.

(50) Delii, J.; Speier, G. *Trans. Met. Chem.* **1981**, *6*, 227-229.

(51) Reynolds, M. S.; Berg, J. M.; Holm, R. H. *Inorg. Chem.* **1984**, *23*, 3057-3062.

(52) Berg, J. M.; Holm, R. H. *J. Am. Chem. Soc.* **1985**, *107*, 925-932.

(53) Caradonna, J. P.; Reddy, P. R.; Holm, R. H. *J. Am. Chem. Soc.* **1988**, *110*, 2139-2144.

(54) Roberts, S. A.; Young, C. G.; Cleland, W. E., Jr.; Ortega, R. B.; Enemark, J. H. *Inorg. Chem.* **1988**, *27*, 3044-3351.

(55) Roberts, S. A.; Young, C. G.; Kipke, C. A.; Cleland, W. E., Jr.; Yamanouchi, K.; Carducci, M. D.; Enemark, J. H. *Inorg. Chem.* **1990**, *29*, 3650-3656.

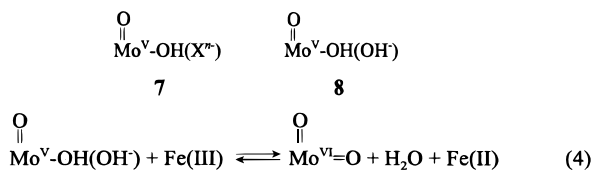
(56) Bhattacharjee, S.; Bhattacharyya, R. *J. Chem. Soc., Dalton Trans.* **1993**, 1151-1157.

(57) Ueyama, N.; Oku, H.; Kondo, M.; Okamura, T.; Yoshinaga, N.; Nakamura, A. *Inorg. Chem.* **1996**, *35*, 643-650.

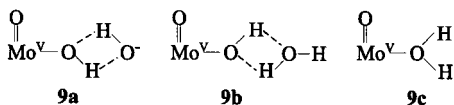
(58) Xiao, Z.; Bruck, M. A.; Enemark, J.; Young, C. G.; Wedd, A. G. *Inorg. Chem.* **1996**, *35*, 7508-7515.

(59) Doonan, C. J.; Slizys, D. A.; Young, C. G. *J. Am. Chem. Soc.* **1999**, *121*, 6430-6436.

because **8**, with an OH⁻ group in the pocket, is preformed for coupled electron proton transfer (CEPT) according to eq 4.



The limiting species (**7** and **8**) were also proposed as the origin of the *hpH* and *lpH* EPR signals produced when SO is reduced chemically by sulfite (species **4** of Figure 5) or photochemically by deazaflavins (species **5** in Figure 5) in the absence of oxidants. Species **7** was assigned to the *lpH* form and **8** to the *hpH* form. Redrawing the *hpH* form as **9a** makes it apparent that hydrogen bonding interactions between the Mo^V-OH group and the OH⁻ in the pocket could result in two protons in close proximity to the Mo atom, as indicated by the RP ESEEM experiments described above. Moreover, these protons could be rotationally distributed, depending upon the orientation of the OH⁻ group in the pocket. Protonation of **9a** gives **9b** which has a water molecule in the pocket. Structures **9a** and **9b** both contain two nearby protons and would not be experimentally distinguishable from a rotationally distributed coordinated water molecule (**9c**) by ESEEM. Structures **9** also explain the paradoxical observation that the *hpH* form of SO apparently has more nearby protons than does the *lpH* form.⁶⁰



The distribution among the proposed *hpH* structures (**9a**–**9c**) will depend on the local pH at the Mo site, which could differ from that of the *hpH* experiment (pH 9.55), and upon the pK_a values of the protons for the various species. For six-coordinate [Ru^{II/III}(OH₂)]ⁿ⁺ complexes, it has been shown that the pK_a of the coordinated water molecule is extremely sensitive to oxidation state and to the π-interactions with the ligands.⁶¹ The oxo-Mo(V) center of SO has an ene-1,2-dithiolate and a S_{cys} ligand. Recent gas-phase PES⁶² and S K-edge XAS⁴⁵ studies for Mo complexes show that these ligands have highly covalent Mo–S bonds that can “electronically buffer”⁶² the Mo center to large changes in charge upon changes in formal oxidation state. It seems reasonable to suggest that another role of the sulfur-rich ligand environment of the Mo center of SO (and other enzymes) is to tune the pK_a of the coordinated H₂O/OH ligand to facilitate CEPT in the oxidative half reaction.

Pilato and Stiefel⁶³ have proposed an alternative mechanism for SO in which a water molecule (or hydroxide ion) that is hydrogen bonded to the equatorial oxo group of the fully oxidized Mo center in a structure similar to **9a** or **9b** becomes activated for incorporation into sulfite to form sulfate. This proposed “outer sphere CEPT-water activation process” cannot be ruled out by the present ESEEM results for the Mo(V) species

(60) Extensive two-pulse and four-pulse ESEEM experiments on the *lpH* form in both D₂O and H₂O buffers showed only a single strongly coupled deuteron (proton) with a unique orientation. Although the presence of a second deuteron (proton) could not be completely ruled out, the possible parameters for a second nucleon are severely restricted (ref 5).

(61) Moyer, B. A.; Meyer, T. J. *Inorg. Chem.* **1981**, *20*, 436–444.

(62) Westcott, B. L.; Gruhn, N. E.; Enemark, J. H. *J. Am. Chem. Soc.* **1998**, *120*, 3382–3386.

(63) Pilato, R. S.; Stiefel, E. I. In *Bioinorganic Catalysis*, 2nd ed.; Reedijk, J., Bouwman, E., Eds.; Marcel Dekker: New York, 1999; p 139.

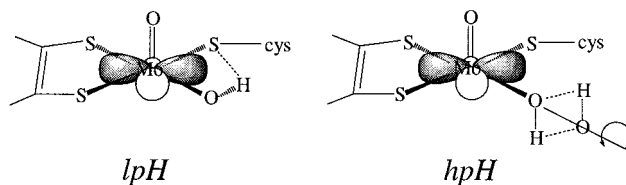
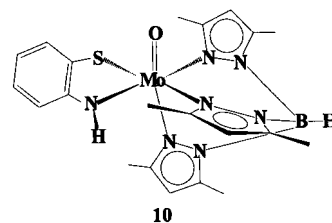


Figure 6. Proposed coordination environments of the Mo(V) centers for the low pH (*lpH*) and high pH (*hpH*) forms of sulfite oxidase. The *lpH* form has a single strongly coupled ordered proton that is ascribed to a Mo–OH···S_{cys} hydrogen bonding interaction in the XY plane. The *hpH* form appears to have two nearby protons in distributed orientations arising from hydrogen bonding between the Mo^V-OH group and a hydroxide ion (or water molecule) in the anion binding pocket (see text).

formed after release of sulfate product (structure **4** of Figure 5). However, the previous observation of significant ¹⁷O hyperfine splittings for the *hpH* and *lpH* forms when the reaction is carried out in H₂¹⁷O enriched water favors the mechanism of Figure 5.⁶⁴ Additional ESEEM experiments that are in progress in ¹⁷O-enriched H₂O should provide further insight concerning the mechanism of SO.

Structures for the *lpH* and *hpH* Forms. The electronic structures of oxo-Mo(V) centers are dominated by the strong Mo=O bond and the unpaired electron is primarily localized in the d_{xy} orbital in the equatorial plane, even in low symmetry complexes.^{65,66} Large isotropic proton hyperfine splittings (~8.3 × 10⁻⁴ cm⁻¹, 25 MHz) are observed for complexes such as (Tp*)MoO(*o*-SC₆H₄NH), Tp* = hydrotris(3,5-dimethyl-1-pyrazolyl)borate (**10**),³⁹ where the steric constraints of the bidentate *o*-SC₆H₄NH ligand place the exchangeable NH proton in the



equatorial plane in a position to directly overlap with the d_{xy} orbital. For the *lpH* form of SO, the large isotropic proton hyperfine splitting (Table 1) strongly suggests that the Mo^V-OH group is oriented so that the proton lies in the equatorial plane where it can have good overlap with the d_{xy} orbital. The fits of the ESEEM spectra of the *lpH* form in D₂O were obtained for a single strongly coupled deuteron with a unique set of parameters that place it close to the XY plane.^{5,60} We postulate that the unique proton orientation of the *lpH* form is due to an intramolecular Mo^V-OH···S_{cys} hydrogen bond (Figure 6, *lpH*). For SO the short equatorial O···S_{cys} distance of 2.8 Å²³ should be favorable for a bent O–H···S hydrogen bond. Hydrogen bonds to coordinated cysteines are a feature of iron sulfur proteins,^{67–70} copper proteins,⁷¹ and heme proteins.⁷² Intramolecular N–H···S hydrogen bonding in [Mo^{VO}(SR)₄]⁻ com-

(64) Cramer, S. P.; Johnson, J. L.; Rajagopalan, K. V.; Sorrell, T. N. *Biochem. Biophys. Res. Commun.* **1979**, *91*, 434–439.

(65) Carducci, M. D.; Brown, C.; Solomon, E. I.; Enemark, J. H. *J. Am. Chem. Soc.* **1994**, *116*, 11856–11868.

(66) Inscore, F. E.; McNaughton, R.; Westcott, B. L.; Helton, M. E.; Jones, R.; Dhawan, I. K.; Enemark, J. H.; Kirk, M. L. *Inorg. Chem.* **1999**, *38*, 1401–1410.

(67) Adman, E. T. *Biochim. Biophys. Acta* **1979**, *549*, 107–144.

(68) Watenpaugh, K. D.; Sieker, L. C.; Jensen, L. H. *J. Mol. Biol.* **1979**, *131*, 509–522.

(69) Adman, E. T.; Sieker, L. C.; Jensen, L. H. *J. Mol. Biol.* **1991**, *217*, 337–352.

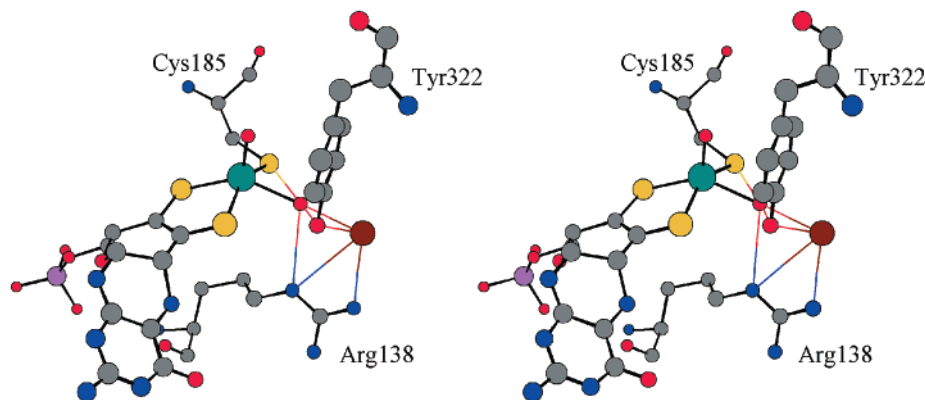


Figure 7. Stereoview of the Mo center of chicken liver SO. The colored lines show the possible hydrogen bonding interactions between the equatorial $\text{Mo}^{\text{V}}\text{-OH}_n$ group and the conserved equatorial ligand (Cys185), the conserved nearby residues Arg138 and Tyr322, and an anion (brown sphere) in the positively charged pocket. In the *hpH* form the anion position is proposed to be occupied by OH^- or a water molecule. Atomic coordinates were taken from the crystal structure of SO.²³

plexes (where SR is an *o*-aminothiolate ligand) is well-documented,⁷³ and the Mo(V/IV) reduction potentials for such complexes are significantly more positive than those for $[\text{Mo}^{\text{V}}\text{O}(\text{SR})_4]^-$ complexes of simple thiolates. No proton hyperfine splittings are observed for the $\text{N-H}\cdots\text{S}$ protons in the CW-EPR spectra of these compounds because the steric interactions among the four bulky SR ligands keep the NH protons out of the equatorial plane. Walters and co-workers have investigated several $(\text{Tp}^*)\text{Mo}(\text{NO})(\text{SR})_2$ compounds in which the R group is an alkane skeleton possessing an amide function.^{74,75} For $\text{R} = \text{SCH}_2\text{CONHCH}_3$ the crystal structure shows an intramolecular $\text{N-H}\cdots\text{S}$ bond with $\text{N}\cdots\text{S} = 2.97 \text{ \AA}$; cyclic voltammetry shows that the reduction potential for this compound is about 300 mV more positive than the potentials for corresponding compounds where R is a simple alkane group. These data from well-characterized Mo-thiolate compounds support the proposed structure for the *lpH* form of SO shown in Figure 6. An alternative orientation for the $\text{Mo}^{\text{V}}\text{-OH}$ group that would also place the proton in the equatorial plane can be achieved by rotating $\sim 180^\circ$ about the Mo-O bond so that the H atom would be in a position to hydrogen bond to the adjacent S atom of the ene-1,2-dithiolate of the pyranopterin. This explanation seems less reasonable for the *lpH* form because this $\text{O}\cdots\text{S}$ distance is 3.2 \AA and, to our knowledge, there are no well-documented cases of H-bonding interactions with coordinated ene-1,2-dithiolate ligands.

We have previously suggested⁵ that the absence of a large isotropic proton hfi for the *hpH* form reflects torsional angle changes about the $\text{Mo}^{\text{V}}\text{-OH}$ bond that move the proton out of the d_{xy} orbital (Figure 6). Here we propose that a strong hydrogen bonding interaction between the equatorial $\text{Mo}^{\text{V}}\text{-OH}$ group and a hydroxide (**9a**) or water molecule (**9b**) in the electrostatic pocket will reorient the $\text{Mo}^{\text{V}}\text{-OH}$ group so that there is no longer a proton in the equatorial plane, thereby eliminating the large isotropic proton hfi. This proposed origin of the differences in the *lpH* and *hpH* EPR spectra is consistent

with the single crystal ENDOR investigation⁷⁶ of a d^1 vanadyl complex with an equatorial water ligand, which showed that a small deviation of the metal-(equatorial proton) vector from the node of a singly occupied ground-state orbital results in a rather large variation of the isotropic constant. For the *hpH* form of SO, structures **9** show a possible explanation for the detection of two nearby protons in this form. However, the total number of nearby protons and their orientations is difficult to specify precisely because the crystal structure of SO indicates that several hydrogen bonding interactions are possible for the equatorial $\text{Mo}^{\text{V}}\text{-OH}$ unit (Figure 7). The $\delta\text{-NH}$ group of Arg138 could serve as a proton donor to the $\text{Mo}^{\text{V}}\text{-OH}$ group ($\text{N}\cdots\text{O} = 3.1 \text{ \AA}$); the oxygen atom of Tyr322, an invariant amino acid in all known SO enzymes, is also within hydrogen bonding distance of the $\text{Mo}^{\text{V}}\text{-OH}$ unit ($\text{O}\cdots\text{O} = 2.6 \text{ \AA}$). Deprotonation of Tyr322 is proposed to be an important aspect of the catalytic cycle.^{29,30} Tyr322 could function as a proton donor or a proton acceptor to the $\text{Mo}^{\text{V}}\text{-OH}$ unit, depending upon the local pH. Thus, the protonation equilibria of Tyr322 could affect both the distribution of $\text{Mo}^{\text{V}}\text{-OH}$ torsional angles and the number of protons detected in the RP ESEEM experiment on the *hpH* form. The unusually small deuterium quadrupole coupling constant found in the *hpH/D}_2\text{O} experiment⁵ suggests at least one uncharacteristically strong hydrogen bonding interaction in the *hpH* form.^{77,78} The *g*-values for the *lpH* and *hpH* forms of SO are surprisingly different (Table 1), considering that the primary difference in the proposed structures (Figure 6) is the torsional angle about the $\text{Mo}^{\text{V}}\text{-OH}$ bond. Preliminary calculations on the electronic structure of the active site of SO indicate that rotation of the equatorial OH group about the $\text{Mo}^{\text{V}}\text{-OH}$ bond can lead to changes in *g*-values as large as 0.01.⁷⁹ The postulated $\text{Mo}^{\text{V}}\text{-OH}\cdots\text{S}_{\text{cys}}$ hydrogen bonding interaction in the *lpH* form may also influence the *g*-values by modulating the donor properties of the coordinated S_{cys} ligand. To our knowledge, there are no data available from well-characterized oxo-Mo(V) compounds to assess this latter possibility.*

The so-called *Pi* EPR spectrum of SO is exhibited in the presence of phosphate⁴⁰ or arsenate³⁴ at low pH. Multi-frequency ESEEM experiments on the *Pi* form²⁰ in phosphate buffer and CW-EPR and EXAFS investigations of SO in the presence of arsenate³⁴ indicate that in these forms a polyoxoanion occupies the anion binding pocket while simultaneously functioning as a monodentate ligand for the equatorial coordination site of SO. Consistent with this structure, the ESEEM spectra of the *Pi* form²⁰ show no detectable modulations from nearby protons (trace 2, Figure 2b).

(70) Backes, G.; Mino, Y.; Loehr, T. M.; Meyer, T. E.; Cusanovich, M. A.; Sweeney, W. V.; Adman, E. T.; Sanders-Loehr, J. *J. Am. Chem. Soc.* **1991**, *113*, 2055–2064.

(71) Guss, J. M.; Freeman, H. C. *J. Mol. Biol.* **1983**, *169*, 521.

(72) Poulos, T. L.; Finzel, B. C.; Howard, A. J. *J. Mol. Biol.* **1987**, *195*, 687.

(73) Ueyama, N.; Okamura, T.; Nakamura, A. *J. Am. Chem. Soc.* **1992**, *114*, 8129.

(74) Huang, J.; Ostrander, R. L.; Rheingold, A. L.; Leung, Y.; Walters, M. A. *J. Am. Chem. Soc.* **1994**, *116*, 6769–6776.

(75) Huang, J.; Ostrander, R. L.; Rheingold, A. L.; Walters, M. A. *Inorg. Chem.* **1995**, *34*, 1090–1093.

The structures proposed for the *lpH* and *hpH* forms of SO in Figure 6 also agree with the CW-EPR experiments on these forms involving ^{17}O -labeling. In H_2^{17}O both the *lpH* and *hpH* forms show ^{17}O hfi that is indicative of exchange of the coordinated OH group in these forms.⁶⁴ However, the ^{17}O hfi parameters are not the same for the two forms. Variation in the $\text{Mo}^{\text{V}}\text{-OH}$ torsional angle and in the number of nearby protons for the two forms will affect the $\text{Mo}\text{-O}$ π -bonding and consequently the ^{17}O hfi parameters and nuclear quadrupole parameters. Additional ESEEM experiments are in progress in ^{17}O -enriched H_2O buffer to distinguish between ^{17}OH and H_2^{17}O ligation using the techniques developed by Thomann et al. to investigate the binding of water to the Fe^{III} center of cytochrome P450_{cam}.⁸⁰

Implications for Sulfite Oxidase Deficiency. Sulfite oxidase deficiency^{81–83} is an inherited metabolic disease that produces severe neonatal neurological disorders, and several fatal point mutations in human SO have been clinically identified.^{23,84} Of particular interest is the point mutation in human SO in which arginine 160 has been replaced by glutamine (R160Q mutation).⁸⁴ This mutant enzyme has only about 2% of the activity of wild type enzyme. This arginine residue is conserved in all SO, and the structure of chicken liver SO shows that it is located in the positively charged anion binding pocket (in chicken SO this is Arg138). The obvious inference is that this mutation interferes with normal sulfite binding and thus disrupts catalysis by slowing down the reductive half reaction that converts **1** to **2** in Figure 5. However, Brody and Hille⁸⁵ have shown that dimethylsulfite, an uncharged molecule, is also a substrate for native SO. Moreover, even though K_{m} and K_{d} are larger for dimethylsulfite than for sulfite, the values of k_{cat} and k_{red} for

the two substrates are not significantly different from one another. Another possible reason for the low activity of the human R160Q mutant is that the changes in the positively charged binding pocket induced by this mutation disrupt the *oxidative* half reaction of the enzyme by altering the subtle hydrogen bonding network that may be essential for reoxidation of the Mo center by CEPT according to eq 4. Future kinetic and ESEEM studies of SO mutants will address this question and should provide further insight concerning the catalytic mechanism of this vital enzyme.

Conclusion

The refocused primary ESEEM technique, together with the multi-frequency capability of our pulsed EPR spectrometer, substantially suppresses the signal from distant protons relative to that from nearby protons and facilitates the direct detection of nearby protons of the *hpH* form of SO that have been previously unobservable by other EPR methods. The numerical simulations of the RP ESEEM spectrum confirm that the nearby protons have distributed hfi parameters, as previous studies in D_2O suggest,⁵ but indicate that those studies somewhat overestimated the anisotropic hfi parameters. This work suggests that there are *two* protons in the vicinity of the Mo^{V} center in the *hpH* form of SO; these are ascribed to strong H-bonding interactions of the $\text{Mo}^{\text{V}}\text{-OH}$ group with other nearby proton donors or to coordinated H_2O rather than OH. The distinctive differences in the CW and pulsed EPR spectra of the *lpH* and *hpH* forms are proposed to result from differences of the $\text{Mo}^{\text{V}}\text{-OH}$ torsional angle and variations in the H-bonding interactions of these two forms. The RP ESEEM technique promises to be widely applicable for the investigation of mutant forms of SO with altered Mo centers and paramagnetic centers in other metalloproteins, where a nearby proton of interest is often masked by much more numerous distant protons and where high spectral resolution is not required.

Acknowledgment. We thank Dr. V. Kozlyuk for invaluable assistance with the pulsed EPR experiments, Mr. Rohit Kedia for assistance with the enzyme purification, and Drs. M. T. Ashby, S. J. N. Burgmayer, J. T. Hazzard, R. Hille, J. McMaster, and E. I. Stiefel for helpful discussions. Financial support from the National Institutes of Health (Grant GM 37773), the National Science Foundation (Grants DIR 9016385 and BIR 922431 for the EPR spectrometer), and the Materials Characterization Program of the University of Arizona is gratefully acknowledged.

JA9916761

(76) Atherton, N. M.; Shackleton, A. J. *Mol. Phys.* **1980**, *39*, 1471–1485.

(77) Soda, G.; Chiba, T. *J. Chem. Phys.* **1969**, *50*, 439–455.

(78) Michal, C. A.; Wehman, J. C.; Jelinski, L. W. *J. Magn. Reson., Ser. B* **1996**, *111*, 31–39.

(79) Neese, F. Private communication.

(80) Thomann, H.; Bernardo, M.; Goldfarb, D.; Kroneck, P. M. H.; Ulrich, V. *J. Am. Chem. Soc.* **1995**, *117*, 8243–8251.

(81) Irreverre, F.; Mudd, S. H.; Heizer, W. D.; Laster, L. *Biochem. Med.* **1967**, *1*, 187–217.

(82) Johnson, J. L.; Rajagopalan, K. V. *J. Clin. Invest.* **1976**, *58*, 551–556.

(83) Johnson, J. L.; Wadman, S. K. In *The Metabolic and Molecular Bases of Inherited Disease*; Scriver, C. R., Ed.; McGraw-Hill: New York, 1995; pp 2271–2283.

(84) Garrett, R. M.; Johnson, J. L.; Graf, T. N.; Feigenbaum, A.; Rajagopalan, K. V. *Proc. Natl. Acad. Sci. U.S.A.* **1998**, *95*, 6394–6398.

(85) Brody M. S.; Hille, R. *Biochim. Biophys. Acta* **1995**, *1253*, 133–135.